PERGAMON

Vision Research 40 (2000) 2437–2447

Vision Research

www.elsevier.com/locate/visres

On the symmetry between eyes of wavefront aberration and cone directionality

Susana Marcos *, Stephen A. Burns

Schepens Eye Research Institute, 20 Staniford Street, Boston, MA 02114, USA

Received 14 July 1999; received in revised form 20 January 2000

Abstract

There are two optical processes that control the retinal image sampled by the photoreceptor array: aberrations of the ocular optics and cone directionality (Stiles–Crawford effect). The shape of wavefront aberration and Stiles–Crawford functions are known to vary markedly across subjects. In this study we investigate in twelve subjects the symmetry between right and left eyes of wavefront aberration (measured using a spatially resolved refractometer) and cone directionality (measured using an imaging reflectometric technique). The pattern of aberrations is in general non-symmetric, suggesting that the development of aberrations follow independent paths in many right and left eye pairs. Cone directionality is in most cases mirror-symmetric (with one case of direct symmetry), suggesting some systematic process underlying cone orientation. Except in two subjects, symmetry in these two functions seems to be unrelated. Cone directionality apodization improves optical quality, but not optimally in all eyes, and it does not tend to increase symmetry in the optical performance of left and right eyes.

Keywords: Wavefront aberration; Cone directionality; Stiles–Crawford effect; Alignment; Symmetry; Optical quality; Human eye

1. Introduction

The image of the world that is available to the photoreceptors depends mainly on three factors: the optical aberrations, photoreceptor topography and cone directionality. Aberrations degrade the optical image projected on the retina, especially for large pupils. The cone-photoreceptors exhibit directional properties so that they funnel the light into the cone outer segments and minimize the capture of stray light. In addition, cone directionality produces a pupil apodization, limiting the effective pupil size, and potentially reducing the impact of aberrations in pupil areas away from the location of maximum luminous efficiency (Atchison, Joblin & Smith, 1998; Burns, He & Marcos, 1998; Zhang, Ye, Bradley & Thibos, 1999). Cone topography controls sampling and we have a fair understanding of its variability (Curcio, Sloan, Kalina & Hendrickson, 1990; Marcos, Navarro & Artal, 1996; Miller, Williams, Morris & Liang, 1996). Ocular aberrations and cone directionality also differ markedly across subjects. Various studies show important inter-subject variability in both the amount and the pattern of ocular aberrations (Howland & Howland, 1977; Walsh, Charman & Howland, 1984; Liang & Williams, 1997; Navarro & Losada, 1997; He, Marcos, Webb & Burns, 1998). Also, psychophysical (Stiles & Crawford, 1933; Applegate & Lakshminarayanan, 1993) as well as reflectometric measurements of cone directionality (Gorrand & Delori, 1995; Burns, Wu, Delori & Elsner, 1996) show that cone orientation (the location at the plane of the pupil towards which the photoreceptors are pointing) also varies significantly across subjects.

Since both the pattern of aberrations and cone directionality vary across subjects, we asked whether these functions are also different between eyes in the same subject, or if on the contrary, these two functions are symmetric between left/right eyes. In this paper we address three main questions: (1) Are aberrations symmetrical between eyes? (2) Is directionality symmetrical between eyes? (3) Do the aberrations and cone direc-

* Corresponding author. Present address: Instituto de Óptica 'Daza de Valdés', Consejo Superior de Investigaciones Cientificas, Serrano 121, Madrid 28006, Spain. Fax: +34-1-5645557.

E-mail address: susana@io.cfmac.csic.es (S. Marcos).

0042-6989/00/$ - see front matter
PII: S0042-6989(00)00103-6

tionality interact similarly in both right and left eyes?. Symmetry will be indicative of a systematic, instead of a random process controlling these functions. Also, optimal performance requires a bilateral optimal interaction between aberrations and cone directionality. That is, by addressing the above questions, we are also asking: (4) Is there a common force driving photoreceptor alignment? (5) Is there a common axis for optics development, along which the cones are oriented and optical quality is best? (6) Is the retina acting like an optimal instrument?

In summary, by studying binocular symmetry of aberrations and cone directionality and the interaction between both functions we are considering (a) the importance of the relative alignment of the aberration and apodization functions for final image quality, and (b) if there might exist some developmental pressure on the eye to coordinate both functions to maximize image quality.

To our knowledge, very few studies in the literature have addressed the issue of symmetry of aberrations or cone directionality between eyes. Liang and Williams (1997) measured the aberrations in the right and left eyes of four subjects, and concluded that they were mirror symmetric across eyes in the same subject. However, the eight eyes in that study had particularly good optical quality (i.e. the aberrations were close to zero), and it is difficult to conclude if this result is general. The optometric literature suggests that marked anisometropia is uncommon, either in the magnitude of sphere or astigmatism (Statterfield, 1989; Almeder, Peck & Howland, 1990). However, optometric measurements of astigmatism in a population of 192 subjects concluded that the axis of astigmatism does not follow any particular rule (mirror or direct symmetry) across right and left eyes (McKendrick & Brennan, 1997). Regarding cone directionality, studies presenting estimates of the Stiles–Crawford effect were generally restricted only to a single eye (Applegate & Lakshminarayanan, 1993) or to right and left eyes of monocularly amblyopic subjects (Enoch, 1959; Delint, Weissenbruch, Berendschot & van Norren, 1998). To our knowledge, only a study by Dunnewold (1964) presented Stiles–Crawford data on both right and left eyes in a group of normal subjects with a large variability in the peak location. His conclusion was that even though the mean peak locations were almost mirror symmetric, the spread of the data was too large to determine the position of the peak location in one eye from the position of the peak location in the fellow eye.

In the current study we present measurements of the wavefront aberration and cone directionality functions in 24 eyes (right and left eyes of 12 subjects). Wavefront aberration was measured using a spatially resolved refractometer (Webb, Penney & Thompson, 1992; He et al., 1998), and cone directionality was measured by means of an imaging reflectometer (Burns et al., 1996). We analyzed the correlation of individual aberrations, and the correlation of global optical quality and optical quality as a function of pupil location, as well as the correlation of cone directionality, in right and left eye of the same subjects. We explored the type of symmetry of these two functions, and if symmetry of optical quality is enhanced when cone directionality is included as an apodization in the modulus of the optical pupil functions.

2. Methods

2.1. Subjects

Twelve normal subjects (seven men and five women, aged 22–58) participated in this study. Both eyes were tested. Spherical refraction ranged from 0 to -6.5 D. Anisometropia was less than 1 D for spherical refraction (except for subject FV, for whom it was 3 D), and less than 0.8 D for astigmatism. Wavefront aberration and cone directionality were collected for one eye in a single session. The second eye was tested in a separate session. The pupil was dilated with tropicamide 0.5%. A typical session lasted less than one hour, including explanation of consent form and fabrication of a dental impression. Average time span between the sessions measuring right and left eyes was 120 days. Cone directionality has been proven to be stable over long periods of time (Rynders, Grosvenor & Enoch, 1995). While wavefront aberrations are known to change with age (Artal, Ferro, Miranda & Navarro, 1993; McLellan, Marcos & Burns, 1999) this occurs over long time periods, and we have found repeat measurements over the course of a year to be quite stable in most adults.

2.2. Measurement of wavefront aberration and optical quality

A spatially resolved refractometer was used to measure wavefront aberration. A detailed description of the technique and experimental procedure can be found elsewhere (He et al., 1998). In this psychophysical technique, the subject aligns a test spot (which enters the pupil of the eye sequentially at 37 locations) to a cross viewed through the pupil center. Both the test and the reference target are green. The pupil is continuously monitored and the pupil center is aligned to the optical axis of the instrument. The refraction is corrected by means of a focusing block. The tilt necessary for the alignment represents the slope of the ocular wavefront aberration at that pupil entry location. The wavefront aberration was estimated using a least square fit of a Zernike polynomial expansion to the tilts up to the seventh order (35 terms). The root-mean-square (RMS)

wavefront error was obtained by adding, appropriately scaled (Noll, 1976), the square of the Zernike coefficients. We obtained optical quality pupil maps by computing the point spread functions (PSF) for a series of 1-mm pupils across the pupil. From these PSFs we calculated the modulation transfer functions (MTF) and the strehl ratio (volume under the MTF normalized to the volume for a diffraction-limited lens) as a function of pupil position. The area of best optical quality in the pupil was determined using a similar procedure. In addition, the volume under the MTF was computed for both a circular pupil (6-mm) and for a Gaussian apodized pupil centered on the subject's cone directionality (see Section 2.3).

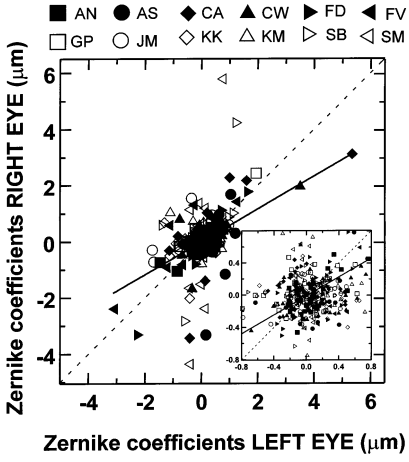

Fig. 1. Zernike coefficients describing the wavefront aberration, for left (abscissa) versus right eyes (ordinate), for 12 subjects. Different symbols represent different subjects. Defocus and tilt terms have been omitted. The inset shows an enlargement of the central part of the plot (coefficients ranging from -0.8 to 0.8 μm). The sign of odd symmetric terms in the right eye have been changed, to test for mirror symmetry. The solid line represents a linear fit to the data. Coefficient of correlation is $r = 0.45$.

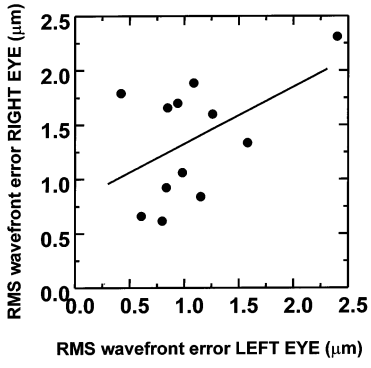

Fig. 2. RMS wavefront error, for left versus right eyes (12 subjects). The solid line represents a linear fit to the data. Coefficient of correlation is $r = 0.5$.

2.3. Measurement of cone directionality

A photoreceptor alignment reflectometer was used to measure cone directionality. This technique has been described in detail previously (Burns et al., 1996). Briefly, in this technique the distribution of the light returning for a 1° area of bleached retina is measured at the plane conjugate to the pupil by means of a high resolution CCD camera. The intensity distribution at the pupil plane is fitted to a gaussian distribution ($A \cdot 10^{-\rho[(x-x_0)^2+(y-y_0)^2]} + B$). The first term represents the light guided back by the photoreceptors. The second term is a constant (B) which accounts for light diffusely reflected that fills the pupil. The coordinates x_0 and y_0 represent the location of maximum reflectance (peak of cone directionality), and are referred to the pupil center. The shape factor ρ is a measure of the width of the intensity distribution.

Images were obtained for different entry positions of the measurement beam, to locate the entry pupil location that produced the brightest guided component (generally producing the best fit). A series of nine images with entry locations forming a 0.5-mm array around the selected location was then obtained. The fitting parameters given below correspond to the image producing the best fit (typically accounting for 85% of the variance of the fit).

3. Results

3.1. Wavefront aberration

The wavefront aberration is represented as a Zernike polynomial expansion up to the seventh order (35 terms). The sequence of our Zernike terms follows the Mahajan (1994) ordering scheme, which for the purposes of this paper is essentially equivalent to the basis used by Malacara (1992). Fig. 1 represents the correlation between Zernike coefficients of right and left eyes (in μm), testing mirror symmetry (i.e. inverting the sign of the odd symmetric terms in the right eye). The inset shows a subset of coefficients ranging from -0.8 to 0.8 μm. Tilt and defocus terms have been omitted. Each symbol type represents a different subject. Coefficients of correlation r of linear fits to the data for each subject range from 0.9 to -0.4. Coefficients of correlation r for repeated measures in the same eye ranged from 0.94 to 0.57. The thick solid line ($r = 0.45$) represents a linear fit to all data in Fig. 1. The correlation between Zernike coefficients of right and left eyes is highly statistically significant ($P < 0.0001$) for mirror symmetry in five subjects (AN, CA, FD, GP and JM). Subject GP also shows a highly significant correlation for direct symmetry. For the rest of the subjects the correlation is not significant for either mirror or direct symmetry.

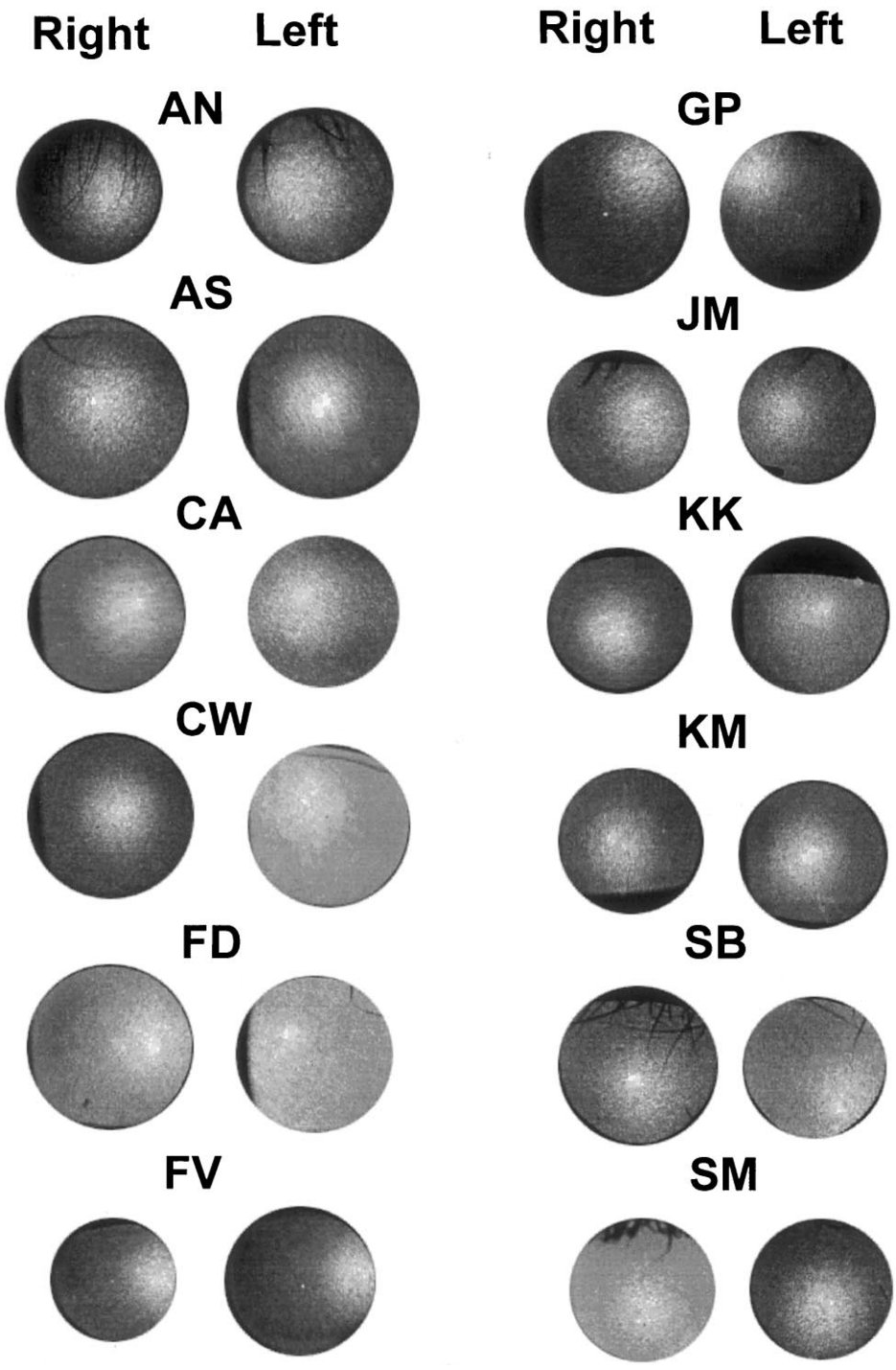

Fig. 3. Intensity distributions at the pupil plane showing cone directionality in right-left eye pairs of 12 subjects. Images are presented as looking toward the subjects' eye, and pupil sizes vary from eye to eye (between 7.2 and 10 mm). The brightest part of the pupil corresponds to light returning from the cone-photoreceptors in a bleached state. Its location varies across individuals, and tends to be mirror symmetric between eyes in the same individuals. Exceptions are FV (showing direct symmetry), SB and CW.

Fig. 2 shows the RMS wavefront error (computed from the Zernike coefficients) for the right eye versus the RMS wavefront error for the left eye, for all subjects. The correlation coefficient r of data in Fig. 2 is 0.5 ($P = 0.1$). For eight out of 12 subjects, the RMS of the most aberrated eye does not exceed 1.5 times the RMS of the fellow eye; for the other three subjects, this factor is less than two. For one subject (SM) the right eye RMS is four times larger than her left eye's RMS. Excluding this subject, the coefficient of correlation r in Fig. 2 increases to 0.7 ($P = 0.02$).

3.2. Cone directionality

Fig. 3 shows the intensity distributions at the pupil plane of light guided back through the pupil when the photopigment is bleached, for right and left eyes of our 12 subjects. The location of the maximum of the intensity distribution represents the pupil position at which the cone photoreceptors are aimed. In many cases the peak of cone directionality is not centered in the pupil, with four subjects (eight eyes) with peaks more than 2 mm from the center of the pupil. Although most eyes tend to be mirror symmetric (GP is the most evident case), we also found one case of very marked direct symmetry (FV), and two cases (SB and CW) of no particular symmetry. Fig. 4 shows the coordinates of the peak of cone directionality in the right eye versus the coordinates of the peak in the left eye, for both horizontal (solid circles) and vertical (open circles) components. Negative coordinates stand for nasal and inferior pupil locations, and positive coordinates stand for temporal and superior pupil locations, respectively. The coefficient of correlation r, including all data in Fig. 4, is 0.4. Whereas the correlation for vertical coordinates ($r = 0.9$) is highly significant ($P < 0.001$), the correlation for horizontal coordinates is low ($r = 0.25$). This correlation is very biased by subject FV, whose peak is 3 mm nasally displaced in the right eye, and 2.5 mm temporally in the right eye. Eight of the subjects have their peaks within 1 mm of one eye with respect to the other, which indicates a great precision in the cone alignment (a displacement of 1 mm is equivalent to an angular deviation of only $\sim 2.5°$). Three subjects (KK,CW and SB) have their peak within 1 and 2.2 mm, and one subject (FV) has his peak separated by 5.5 mm. Excluding this last subject showing direct symmetry, the coefficient of correlation r in Fig. 4 increases to 0.8, being statistically significant ($P < 0.001$) for mirror symmetry.

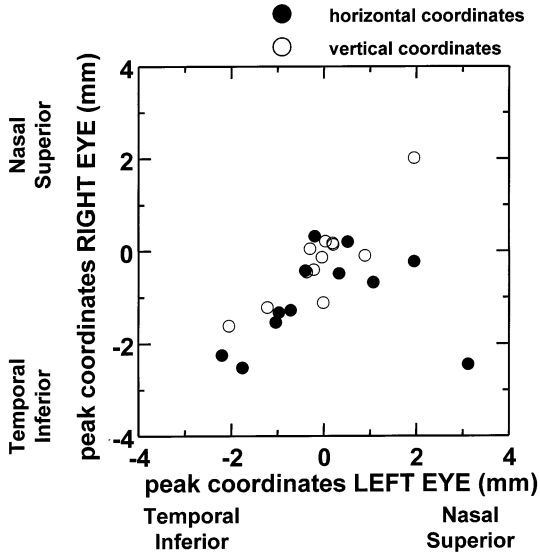

Fig. 4. Coordinates of the maximum of the gaussian function fit to the intensity distribution of light returning from the cones, left versus right eye (12 subjects). Solid symbols represent horizontal coordinates. Open symbols represent vertical coordinates. The coefficient of correlation r, including all data in Fig. 4, is 0.4 ($r = 0.9$ for vertical coordinates and 0.25 for horizontal coordinates). Excluding the outlying subject (FV) correlation increases to 0.7.

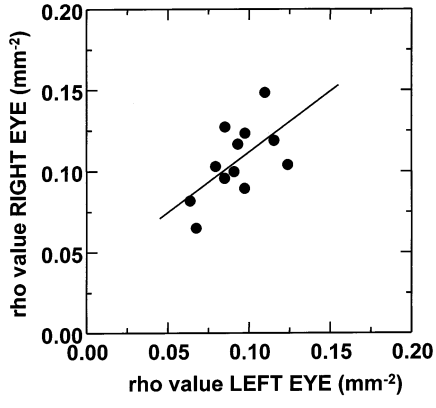

Fig. 5. Shape factor ρ of the gaussian distribution gaussian function fitting the intensity distribution of light returning from the cones, left versus right eye (12 subjects). The solid line represents a linear fit to the data. Coefficient of correlation is $r = 0.7$.

The other parameter that describes the gaussian distribution of light guided by the cone-photoreceptors is the shape factor ρ. Fig. 5 shows ρ values for right eyes versus ρ values for left eyes in the group of 12 subjects. The correlation coefficient r is 0.7 ($P = 0.03$).

4. Discussion

We have shown that the ocular aberrations are mirror symmetric between right and left eye in five out of 12 subjects, and the RMS is comparable between eyes in eight out of 12 subjects. Cone directionality is often mirror symmetric between right and left eyes, with only two cases with no apparent symmetry and one case of direct symmetry. While conclusions are restricted by the limited number of subjects, we will show that there are several statistically significant trends detectable, even with the relatively low statistical power available from a 12 subject/24 eye study.

In the following subsections we analyze the pupil pattern of optical quality in both right and left eye and compare the location of best optical quality within the pupil, to the location of the cone directionality peak. We also study the interaction between optical quality and cone directionality. We finally discuss the implications of these findings.

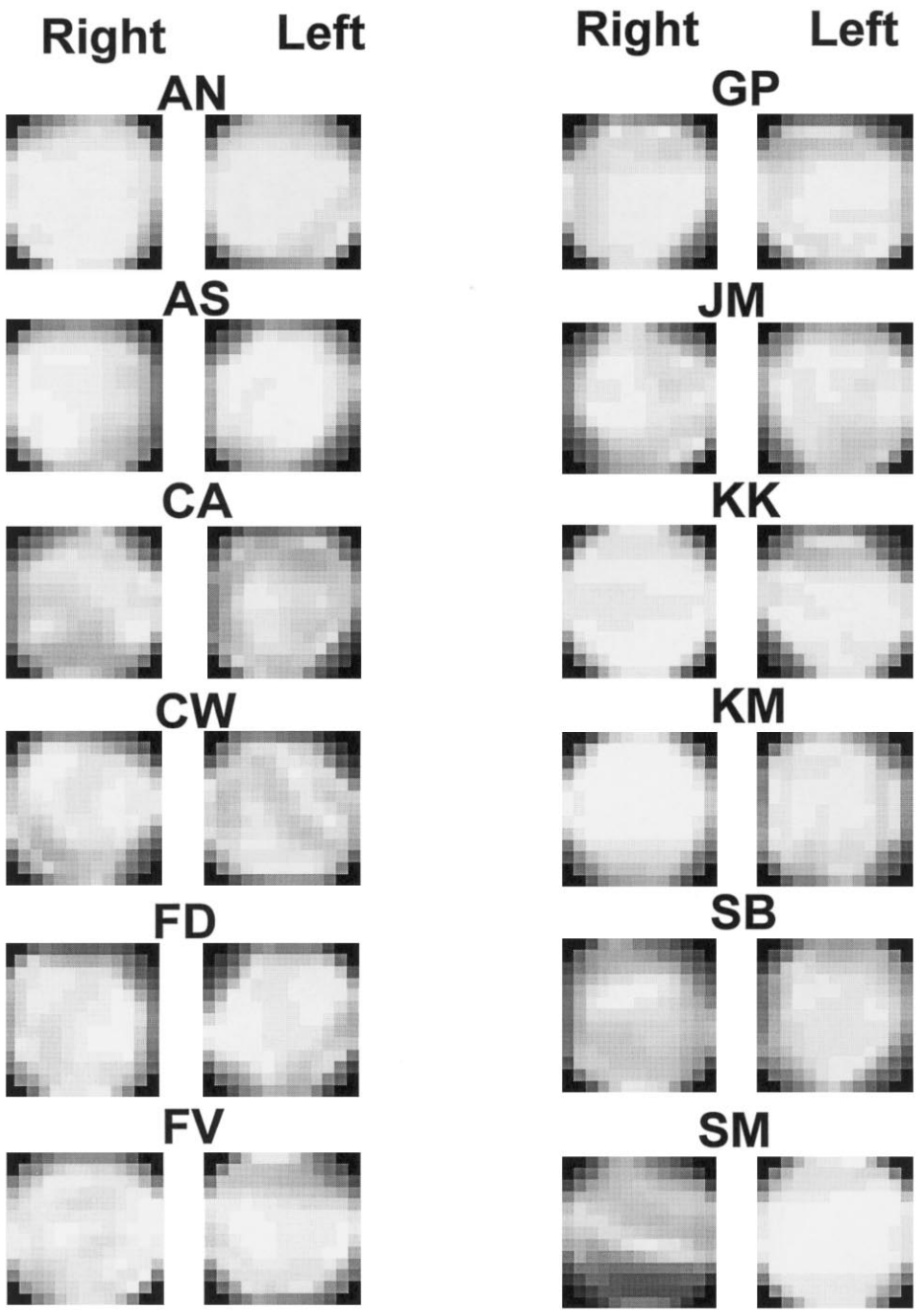

Fig. 6. Maps representing the pattern of optical quality across the pupil. Images are presented as looking toward the subjects' eye. The grayscale of each pixel represents a local strehl ratio, for a 1-mm pupil located at the corresponding pupil location (0.5 mm steps). Brighter parts of the pupil correspond to areas of better optical quality.

4.1. Comparison of optical quality and cone directionality

The correlation between Zernike coefficients of right versus left eye indicates the similarity of individual aberrations between eyes. However, they do not show which areas of the pupil exhibit better optical quality, or the symmetry of the pattern of optical quality within the pupil between right and left eye. Fig. 6 shows optical quality pupil maps, for right and left eyes of the 12 subjects. Each pixel represents a pupil location, and its gray scale represents the local strehl ratio, for a 1-mm pupil centered on that location. Darker regions indicate pupil areas of poorer optical quality, whereas white regions indicate diffraction limited performance for a 1-mm pupil. We observe that for eyes with few aberrations (i.e. subject AN both eyes, subject SM left eye), the central region of the pupil is diffraction-limited for 1-mm pupils, and only becomes degraded at the

pupil edges. However, most pupil maps show a very irregular pattern, differing between right and left eye of the same subject. In many cases, the lack of symmetry between eyes is qualitatively apparent in the pupil maps of Fig. 6 (i.e. subjects CW, SB, SM). However, it is difficult to establish which is the area of the pupil showing best optical quality, to assess if that location corresponds to a symmetric pupil area in the fellow eye, and if the region of best optical quality corresponds to the maximum of cone directionality.

To determine quantitatively the best optical region of the pupil, we repeated the calculations of Fig. 6, but using larger pupil masks (2 mm diameter). The corresponding pupil maps enhance the irregularity of the pattern but reveal basically the same features. In this analysis, we consider nine pupil areas tiling the entire pupil, with a 2-mm center-to-center spacing. The area with the highest strehl ratio was taken as our estimate of the region with best optical quality. Fig. 7a shows the nine pupil areas as outlined within a 6-mm pupil. Each subarea contains the initials of the subjects showing best optical quality in that area. R stands for right eye and L stands for left eye. For five out of 12 subjects, the pupil area with best optical quality is the same in right and left eye (note that not all these subjects have a significant correlation between Zernike coefficients). Fig. 7b shows a similar pupil division, but now the initials of the subjects whose peak of cone directionality falls in that area. For eight out of 12 subjects, the same pupil area contains the peak of cone directionality for both right and left eyes. Fig. 7b shows the tendency of cone orientation toward centered and nasal pupil locations (16 out of 24 eyes), which is not evident for the area of best optical quality (12 out of 24 eyes are better in centered or nasal region). Finally, for seven eyes the region of the pupil for best optical quality corresponds to the region of maximum cone directionality. Among these seven eyes, only four eyes are left/right pairs (subjects FD and CA).

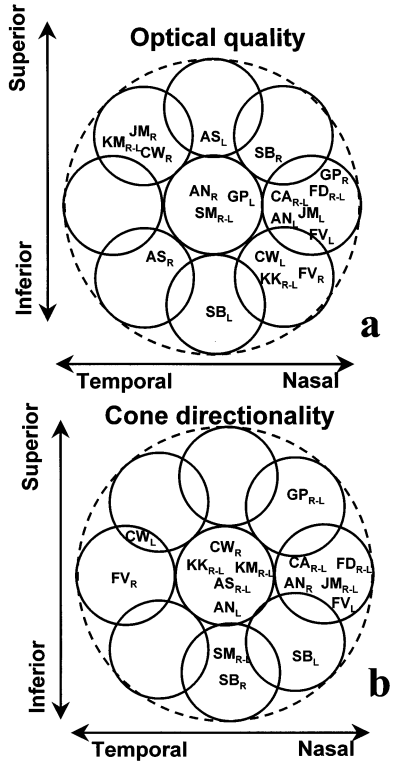

Fig. 7. Pupil division showing the region containing the maximum of (a) best optical quality and (b) cone directionality, for each of the subjects (represented by their initials). R stands for right and L for left eye. R–L pairs are indicative of mirror symmetry. There are five R–L pairs for optical quality and eight for cone directionality. The region of best optical quality and maximum cone directionality agrees in seven eyes, four of them being eye pairs (subjects FD and CA).

4.2. Interaction between optical quality and cone directionality

In the previous section we compared the pupil area containing the maximum of cone directionality, with the pupil area with best optics. However, apodization could be most effective not near its peak, but in the attenuation of luminosity in areas of the pupil far from the cone directionality peak. To test this we computed the local strehl ratio for 2-mm sample pupils at nine locations tiling the pupil (as in Fig. 7) and the average luminosity produced by cone directionality for the same regions. Since the shape factor ρ from single-entry reflectometric measurements is narrower than the shape factor expected only from waveguide properties, we have considered $\rho = 0.1$ mm^{-2} for all subjects (Marcos, Burns & He, 1998; Marcos & Burns, 1999; He, Burns & Marcos, 1999). We did this by stratifying each of the nine subregions of the pupil into either a high luminosity, a moderate luminosity, or a low luminosity group. The average strehl ratio was greater for regions of high luminosity than for regions of low luminosity (ANOVA, Scheffe test, $P < 0.01$). The overall analysis indicates that on average, areas near the peak of the luminosity function are optically better than regions far from the peak. In fact this same trend is seen for regions with intermediate luminosity, which have a higher strehl ratio than regions with low luminosity ($P < 0.05$). It should be stressed that while this trend was present, it was not true for every eye. To evaluate this we also correlated luminosity and strehl ratio for each pupillary region, for each eye. The measured coefficients of correlation r ranged from 0.79 to -0.72. A high positive correlation is indicative of an optimized interaction between aberrations and cone directionality, and a low or negative correlation is indicative of a mismatch between both functions. Taken one at a time, we found 4 eyes with a significant positive correlation: AS, left eye ($r = 0.69$, $P = 0.03$); FD, right eye ($r = 0.79$; $P = 0.007$); FV, right eye ($r = 0.71$, $P = 0.02$); and SB,

left eye ($r = 0.78$; $P = 0.01$), and two eyes with a significant negative correlation: GP, left eye ($r = -0.76$; $P = 0.01$) and SB, right eye ($r = -0.72$; $P = 0.04$). While there is no significant correlation between local strehl ratio and luminosity in the rest of the eyes, these statistics are limited by the small number of pupil samples (nine).

Finally, we investigated if, regardless of the relative location of best optics and directionality peak, cone directionality limits the effective area of the pupil, and reduces the impact of aberrations. The results of several studies in the literature based on computer simulations are controversial as to the effect of the Stiles–Crawford effect on the modulation transfer function (MTF). Van Meeteren (1974) calculated only minor effects of the SCE on the MTF for a 5-mm pupil diameter, whereas Atchinson's (1984) model (using an 8-mm pupil diameter) predicted a larger effect. More recent studies have shown that the effect depends markedly on the amount of aberrations and the exact peak location of cone directionality for a particular subject (Burns et al., 1998). In addition, in order to determine whether cone directionality interacts with the aberrations to increase the symmetry in optical quality between eyes, we have computed PSFs and MTFs, with and without the apodization effect of cone directionality for each particular subject. Fig. 8 shows PSFs for right and left eyes, for a 6-mm pupil, when cone directionality is introduced. These PSFs include astigmatism, but not defocus. We observe that the PSFs differ significantly from right to left eye. Fig. 9 shows the log of the volume under the MTF, for a 6 mm pupil, of right eyes versus left eyes in the group of 12 subjects, for a circular pupil (open circles) or a gaussian mask centered at the peak of cone directionality, with a 6-mm maximum pupil (solid circles). We found a linear relationship (with negative slope) between RMS and log volume under MTF ($r = 0.946$). Therefore, to make Fig. 9 more comparable to Fig. 5, we represent log volume instead of linear volume. Figure (9) shows that for all subjects, the volume under the MTF increases when introducing cone directionality (i.e. the optical quality improves). However, the coefficient of correlation between right and left eyes for the data including cone directionality ($r = 0.35$) is similar than the correlation for the data not including cone directionality ($r = 0.40$).

4.3. Implications of our results

We have found a larger tendency for cone directionality than for ocular aberrations to be mirror symmetric. The presence or lack of symmetry in the optical quality does not seem in general to be correlated with the presence or lack of symmetry in cone directionality. Although, for some eyes the maximum of cone directionality corresponds to the area of the pupil of best optical quality, that does not seem to be the general rule. Taken all data together, the average local strehl ratio is significantly higher for regions of high luminosity (close to the cone directionality peak) than for regions of low luminosity, although individually, the correlation is only significant in four eyes. We have only found two eye pairs, with the same symmetry in both cone directionality and optical quality (in both cases, both right and left eyes show a nasal decentration of both functions).

The fact that in most eyes, cones point toward mirror symmetric pupil locations suggests some sort of systematic mechanism for cone orientation. Some findings in the literature, like cone realignment following retinal detachment (Enoch, Van Loo & Okun, 1973), or after recovery from other retinal conditions (Smith, Pokorny, Ernest & Starr, 1978) suggest that this mechanism may be active. Phototropism has been suggested as a potential control mechanism mediating cone orientation, supported by data that show a change in retinal directional sensitivity with displaced natural pupils (Dunnewold, 1964; Bonds & MacLeod, 1978) or artificial pupils decentered from the SCE peak (Applegate & Bonds, 1981). We have found that in 25% of the subjects we tested, cone directionality peak locations are further than 2 mm from the pupil center. At least in these eyes, in which the pupil location of maximum luminous efficiency gets blocked by the iris in typical daylight conditions, cone orientation does not seem to be light-driven. Retinal-based tractional forces have also been proposed to influence cone alignment (Enoch, 1975). Enoch and Birch (1980) explained the bilateral nasal shift of cone directionality in one of their subjects by stress originating at the blind spot in the subject's two eyes. Whatever the mechanism, it does not operate similarly in all subjects, since we have found particular cases of both asymmetry and direct symmetry. The fact that the shape factor ρ is similar in right and left eye of the same subject indicates that the factors determining the widths of the cone directionality intensity distributions are similar in both eyes. In normal eyes, these factors are the waveguide properties of the cone-photoreceptors (given by the structural properties of the cones and indices of refraction) and cone spacing and aperture (Marcos et al., 1998; Marcos & Burns, 1999).

Aberrations are generally not the same in right and left eyes. This indicates that alignment of the ocular components, and the structure of cornea and lens seem to follow independent paths in right and left eyes, and in most subjects there is not a privileged axis in the eye for both cone orientation and ocular components. Burns et al. (1998) suggested the possibility that the cone photoreceptors might be pointing toward areas of good optical quality in the pupil. That seems to be the case for two eye pairs, and three other individual eyes. It is true that cones tend to avoid pointing toward very degraded pupil areas: Following the same approach as

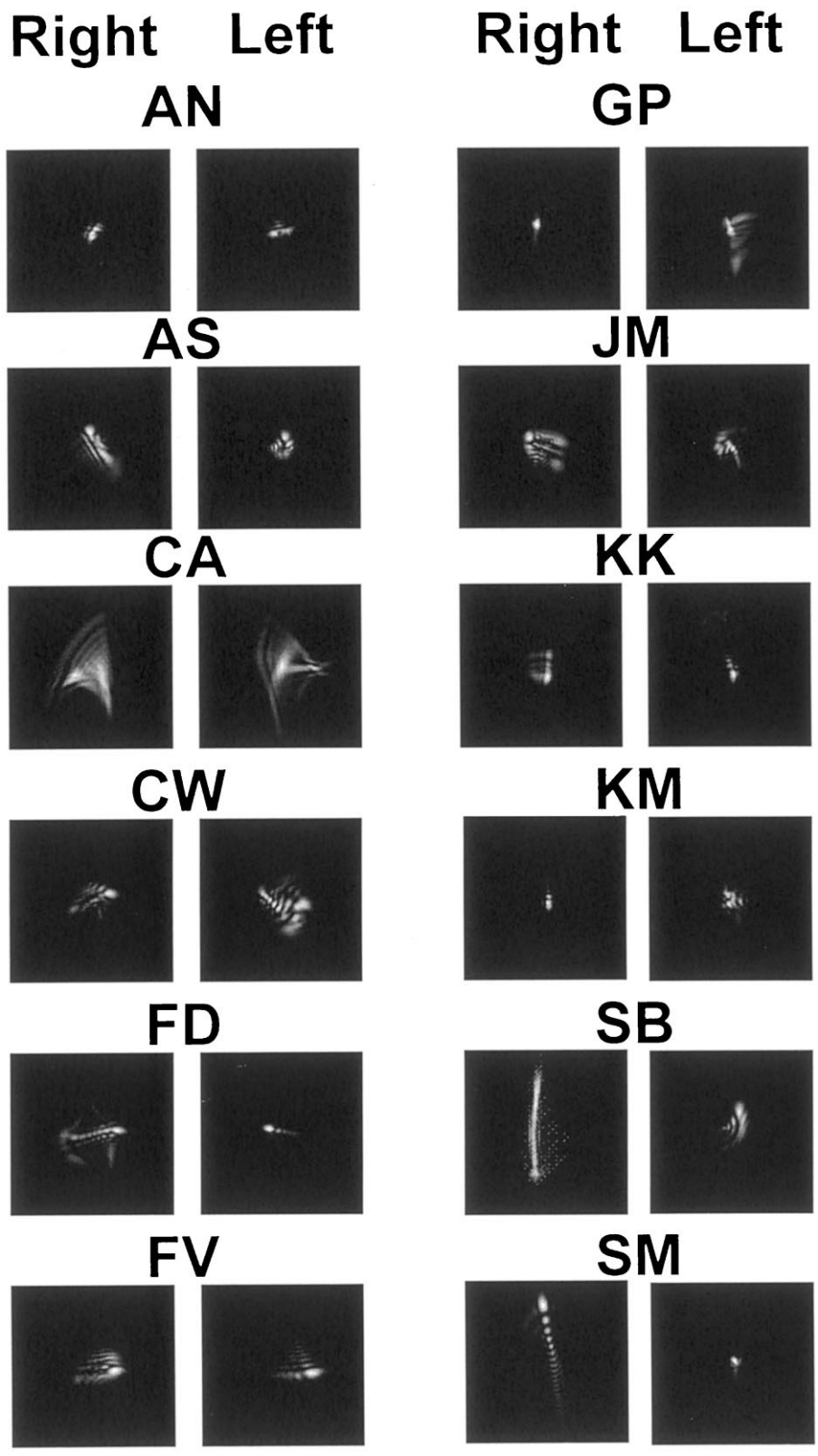

Fig. 8. Point spread functions (PSFs), for right and left eyes in 12 subjects, computed from the wavefront aberrations for 6-mm pupils, and a gaussian apodization corresponding to the subject's own cone directionality.

used in Fig. 7, we never found cone directionality peaks falling within the subregion of the pupil with the worst optics (lowest strehl ratio). From the overall analysis we found that, on average, areas near the peak of the luminosity function are optically better than regions far from the peak. However, for individual eyes, we cannot state that there is a correlation between optical degradation and Stiles–Crawford luminosity attenuation across the pupil. This finding is in agreement with our observation that cones are not in general pointing toward the foveal achromatic axis (Marcos, Burns, Moreno-Barriuso & Navarro, 2000). These results rule out the presence of an accurate feedback mechanism between cone alignment and the optical axis, or a common evolutionary pressure that coordinates accurately apodization and aberrations (in a way similar to 'emmetropization' to control defocus). Although our results do not show an accurate match between optical quality and cone orientation, it remains to be seen if after a drastic change of the pattern of aberrations (i.e. trauma, refractive surgery, etc.) a change in cone directionality is observed. This would not solve the question of how the cones could select pupil areas with best optical quality, or why they would point (in cases of eccentric alignment) to pupil areas blocked by the iris under normal daylight conditions.

In summary, from the previous findings we can answer the questions that we addressed in Section 1: (1) The pattern of aberrations and optical quality is not symmetric between right and left eye, in general. (2) Cone directionality tends to be mirror symmetric between right and left eye. (3) The interaction between aberrations and cone directionality results in an improvement of optical quality, but not in an increase in symmetry. (4) There seems to be a common force driving cone orientation in right and left eyes, although the nature may be different across subjects. (5) Our data do not support the existence of a common axis for optics development, along which the cones are oriented and optical quality is best. (6) The fact that cone directionality apodization does not always occur at the optically best pupillary region and the lack of bilateral symmetry in retinal image quality suggests that in general the ocular optics and cone alignment do not develop toward an optimal optical design.

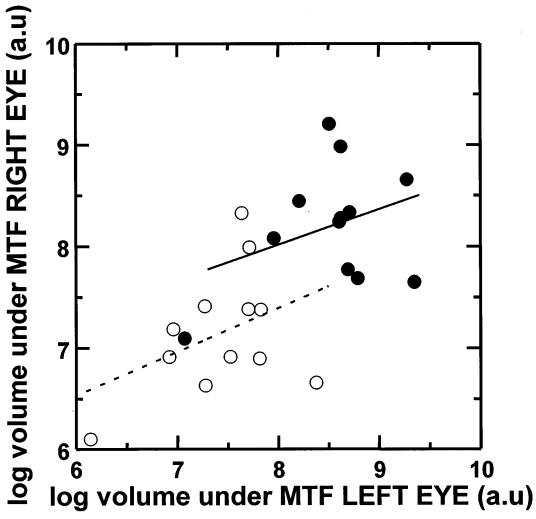

Fig. 9. Log volume under the MTF, for right versus left eye for 6-mm pupils, not including cone directionality (open symbols), and including each subject's own cone directionality (filled symbols). Dashed and solid lines represent linear fits to the data. Coefficient of correlation are $r = 0.4$ and 0.35, respectively.

Acknowledgements

Authors acknowledge support of NIH grant EYO4395, Department of Energy Center of Excellent grant DE-FG-02-91ER61229 and Human Frontier Science Program LT-542/97.

References

Almeder, L. M., Peck, L. B., & Howland, H. C. (1990). Prevalence of anisometropia in volunteer laboratory and school screening populations. *Investigative Ophthalmology and Vision Science*, *31*, 2448–2455.

Applegate, R. A., & Lakshminarayanan, V. (1993). Parametric representation of Stiles–Crawford functions: normal variation of peak location and directionality. *Journal of the Optical Society of America A*, *10*, 1611–1623.

Applegate, R. A., & Bonds, A. B. (1981). Induced movement of receptor alignment toward a new pupillary aperture. *Investigative Ophthalmology and Vision Science*, *21*, 869–872.

Artal, P., Ferro, M., Miranda, I., & Navarro, R. (1993). Effects of aging in retinal image quality. *Journal of the Optical Society of America A*, *10*, 1656–1662.

Atchison, D. A. (1984). Visual optics in man. *Australian Journal of Optometry*, *67*, 141–150.

Atchison, D. A., Joblin, A., & Smith, G. (1998). Influence of Stiles–Crawford apodization on spatial visual performance. *Journal of the Optical Society of America A*, *15*, 2545–2551.

Bonds, A. B., & MacLeod, D. I. A. (1978). A displaced Stiles–Crawford effect associated with an eccentric pupil. *Investigative Ophthalmology and Vision Science*, *17*, 754–761.

Burns, S. A., He, J. C., & Marcos, S. (1998). The influence of cone directionality on optical image quality. *Investigative Ophthalmology and Visual Science* (*Supplement*), *39*, 203.

Burns, S. A., Wu, S., Delori, F. C., & Elsner, A. E. (1996). Direct measurement of human cone-photoreceptor alignment. *Journal of the Optical Society of America A*, *12*, 2329–2338.

Curcio, C. A., Sloan, K. R., Kalina, R. E., & Hendrickson, A. E. (1990). Human photoreceptor topography. *Journal of Comparative Neurology*, *292*, 497–523.

Delint, P. J., Weissenbruch, C., Berendschot, T. T., & van Norren, D. (1998). Photoreceptor function in unilateral amblyopia. *Vision Research*, *38*, 613–617.

Dunnewold, C. J. W. (1964). *On the Campbell and Stiles–Crawford effects and their clinical importance*. Ph.D. Dissertation, Rijuniversiteit Utrecht.

Enoch, J. M., Van Loo Jr, J. A., & Okun, E. (1973). Realignment of photoreceptors disturbed in orientation secondary to retinal detachment. *Investigative Ophthalmology*, *12*, 849–853.

Enoch, J. M., & Birch, D. G. (1980). Evidence for alteration in photoreceptor orientation. *Ophthalmology*, *87*, 821–834.

Enoch, J. M. (1975). Marked accommodation, retinal stretch, monocular space perception, and retinal receptor orientation. *American Journal of Optometry and Physiological Optics*, *52*, 376–392.

Enoch, J. M. (1959). Receptor amblyopia. *American Journal Ophthalmology*, *48*, 262–273.

Gorrand, J. M., & Delori, F. C. (1995). A reflectometric technique for assessing photoreceptor alignment. *Vision Research*, *35*, 999–1010.

He, J. C., Burns, S. A., & Marcos, S. (1999). Cone photoreceptor directionality from reflectometric and psychophysical measurements. *Journal of the Optical Society of America A*, *16*, 2363–2369.

He, J. C., Marcos, S., Webb, R. H., & Burns, S. B. (1998). Measurement of the wave-front aberration using a fast psychophysical procedure. *Journal of the Optical Society of America A*, *15*, 2449–2456.

Howland, H. C., & Howland, B. (1977). A subjective method for the measurement of monochromatic aberrations of the eye. *Journal of the Optical Society of America*, *67*, 1508–1518.

Liang, J., & Williams, D. R. (1997). Aberrations and retinal image quality of the normal human eye. *Journal of the Optical Society of America A*, *14*, 2873–2883.

Mahajan, V. N. (1994). Zernike circle polynomials and optical aberrations of systems with circular pupil. *Applied Optics*, *33*, 8121–8124.

Malacara, D. (1992). *Optical shop testing* (p. 465). New York: Wiley.

Marcos, S., Burns, S. A., Moreno-Barriuso, E., & Navarro, R. (2000). A new approach to the study of ocular chromatic aberrations. *Vision Research*, *39*, 4309–4323.

Marcos, S., & Burns, S. A. (1999). Cone spacing and waveguide properties from cone directionality measurements. *Journal of the Optical Society of America A*, *16*, 995–1004.

Marcos, S., Burns, S. A., & He, J. C. (1998). A model for cone directionality reflectometric measurements based on scattering. *Journal of the Optical Society of America A*, *15*, 2012–2022.

Marcos, S., Navarro, R., & Artal, P. (1996). Coherent imaging of the cone mosaic in the living human eye. *Journal of the Optical Society of America A*, *13*, 897–905.

McLellan, J. S., Marcos, S., & Burns, S. A. (1999). The change of the aberrations of the eye with age. *Investigative Opthalmology and Visual Science* (*Supplement*), *40*, 36.

McKendrick, A. M., & Brennan, N. A.. (1997). The axis of astigmatism in right and left eye pairs. *Optometry and Vision Science*, *74*, 668–675.

Miller, D. T., Williams, D. R., Morris, G. M., & Liang, J. (1996). Images of the cone photoreceptors in the living human eye. *Vision Research*, *36*, 1067–1079.

Navarro, R., & Losada, M. A. (1997). Aberrations and relative efficiency of light pencils in the living human eye. *Optometry and Visual Science*, *74*, 540–547.

Noll, R. J. (1976). Zernike polynomials and atmospheric turbulence. *Journal of the Optical Society of America*, *66*, 207–211.

Rynders, M. C., Grosvenor, T., & Enoch, J. M. (1995). Stability of the Stiles–Crawford function in a unilateral amblyopic subject over a 38-year period: a case study. *Optometry and Visual Science*, *72*, 177–185.

Smith, V. C., Pokorny, J., Ernest, J. T., & Starr, S. J. (1978). Visual function in acute posterior multifocal placoid pigment epitheliopathy. *American Journal of Ophthalmology*, *85*, 192–199.

Statterfield, D. S. (1989). Prevalence and variation of astigmatism in a military population. *Journal of the American Optometry Association*, *60*, 14–18.

Stiles, W. S., & Crawford, B. H. (1933). The luminous efficiency of rays entering the eye pupil at different points. *Proceeding Royal Society of London B*, *112*, 428–450.

Van Meeteren, A. (1974). Calculations of the optical modulation transfer function of the human eye for white light. *Optica Acta*, *21*, 395–412.

Walsh, G., Charman, W. N., & Howland, H. C. (1984). Objective technique for the determination of the monochromatic aberrations of the human eye. *Journal of the Optical Society of America A*, *1*, 987–992.

Webb, R. H., Penney, C. M., & Thompson, K. P. (1992). Measurement of the ocular wavefront distortion with a spatially resolved refractormeter. *Applied Optics*, *31*, 3678–3686.

Zhang, X., Ye, M., Bradley, A., & Thibos, L. N. (1999). Apodization by the Stiles–Crawford effect moderates the visual impact of retinal image defocus. *Journal of the Optical Society of America A*, *16*, 812–820.